Proceedings of the IASS 2024 Symposium
Redefining the Art of Structural Design
August 26-30, 2024, Zurich Switzerland
Philippe Block, Giulia Boller, Catherine DeWolf,
Jacqueline Pauli, Walter Kaufmann (eds.)

Experiment on the structural behaviour of tri-layer and two-chamber ETFE cushion

Xuetao Zhao[a], Bing Zhao[a], Wujun Chen[a, b,] *, Jing Cai[c], Ying Zhang[c]

* Structure Research Center, Shanghai Jiao Tong University, Shansghai, 200240, PR China
800. Dongchuan Road, Shanghai Jiao Tong University, Shanghai, PR China
cwj@sjtu.edu.cn

[a] Structure Research Center, Shanghai Jiao Tong University, Shansghai, 200240, PR China
[b] Shanghai Key Laboratory for Digital Maintenance of Buildings and Infrastructure, Shanghai Jiao Tong University, Shanghai 200240, PR China
[c] Shanghai Taiyokogyo Co., Ltd, Shanghai, 200240, China

Abstract

Since the conventional double-layer ETFE cushion proves inadequate in meeting the structural strength requirements under extreme weather conditions, a double-outer-layer has been proposed as a strengthening alternative for the conventional single outer layer, forming a tri-layer and two-chamber cushion to enhance the structural performance. However, rare empirical engineering knowledge largely dominates the structure design, as performance enhancement mechanism and the load carrying mechanism of the double-outer-layer remains unclear and there is no solid research published yet. This paper will firstly report the experimental results of tri-layer and two-chamber ETFE cushion structure under progressive suction load. Loading test have been designed and performed on two 1.5×1.5 m square tri-layer and two-chamber ETFE cushions. A classic micro-openings design has been adopted in specimens design in alignment with engineering structure. Progressive suction test was conducted at room temperature. An experiment system is developed, consisting of a 1.5m×1.5m×1.8m thin-walled steel loading compartment, and a loading pneumatic control module capable of applying normal suction loading to the cushion surface. Deformation and overall envelop geometry are measured using photogrammetry and laser meteor, while a cushion pressure control module regulates and monitors the chamber pressure of the cushion. Experiment results demonstrate that the pressure difference between chambers exhibits strong correlation with structural performance of tri-layer and two-chamber cushion structure. With greater pressure gradient among chambers, enhanced structural performance is observed in chamber pressure gradient development, decrease surface deformation and failure mode shift. This study provides valuable insights into the understanding of performance enhancement mechanism and inspiration on further research.

Keywords: tri-layer ETFE cushion, chamber pressure gradient, progressive suction load, structural behaviour, structure deformation, ultimate bearing capacity, failure mode

1. Introduction

ETFE (ethylene-tetrafluoroethylene), a copolymer material synthesized with ethylene and tetrafluoroethylene (TFE)[1], boasts a range of exceptional properties. These properties include outstanding light transmission, impressive physical attributes [2], lightweight nature[3], and substantial mechanical properties[4]. This makes ETFE foil a popular building material in both environmental and aesthetical constructions[5]. The utilization of ETFE membrane structures was first realized in 1982[6], and since then, it has gained immense popularity in civil engineering.

The cushion form is the most prevalent configuration in the application of ETFE foils[7]. In this configuration(see Figure 1), multiple layers of ETFE foil are heat-sealed around the perimeter and securely clamped within a frame [2], [7]. Upon inflation with pressurized air to a specific internal pressure, this configuration yields a stable ETFE cushion with exceptional load-bearing capabilities.

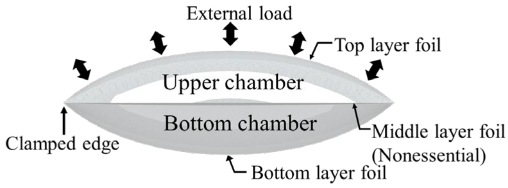

Figure 1. Typical structural scheme of ETFE cushion

The structural strength of cushion is the most crucial factor for engineering applications. As ETFE cushion structure received enormous attention from worldwide, growing demand for ETFE cushion with enhanced strength has come into reality. Conventional double-layer cushion with ETFE foil of regular thickness(100µm-250µm) exhibits insufficient strength performance under extreme weather conditions, such as the hurricanes, strong sandstorms, and typhoons.

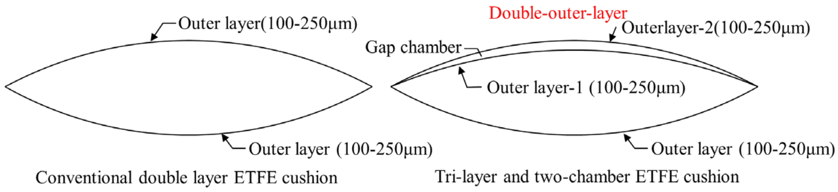

Figure 2. Structural form of multiple layer ETFE cushion

A prevalent and cost-effective method to address above problem is double-outer-layer – attaching another ETFE foil of regular thickness to existing layers with a chamber gap (see Figure 2). Instead of withstanding loads with one solely single layer, the double-outer-layer ETFE foils engage in co-working, collectively bearing the load. With considerable strength enhancement and relative low expense, this structure type stands out as the primary choice and has found application in numerous engineering projects worldwide, such as The Shed at Hudson yards in New York, USA[8] (see Figure 3(a)), Lakhta Centre in St. Petersburh, Russia [9](see Figure 3 (b)), the Grugapark botanical gardens project in Essen, Germany[10] (see Figure 3 (c)) and the infinitus square[11] in Guangzhou, China (see Figure 3 (d)). These projects are commonly featured with multiple layers cushion structure, where traditional single layer is replaced with double-outer-layer on single or both sides of cushion.

Despite the growing applications of ETFE cushion with multiple outer layers, their specific effects on the structural performance of the cushion remain unclear, and there are no publicly available reports addressing this aspect. Consequently, in current engineering projects, the adoption of multiple layer designs primarily guided by past engineering experiences due to a lack of comprehensive knowledge on the nuanced interplay between chamber pressure and cushion structural performance.

Among the various loads encountered in the design process of ETFE cushions, wind suction load is undoubtedly the most critical one. It is because the orientation of the suction load is mostly aligned with the cushion internal pressure and posing a potential risk of ETFE film failure. Therefore, investigating the structural behaviour of ETFE cushions under wind suction loads is not only crucial but also a necessary undertaking.

This study marks the first experimental exploration of the structural behaviour of tri-layer and two-chamber ETFE cushions subjected to suction. Two tri-layer and two-chamber ETFE cushion specimens in square shape, each with classic structural design in different size were manufactured. An integrated experimental system was developed, comprising ETFE cushion specimens, a load simulation system, and a measurement system. Progressive suction tests were conducted on specimens at room temperature.

The tests focused on capturing variations in cushion chamber pressure, surface deformation, ultimate bearing capacity and failure mode between the two specimens. Stress and strain distribution of two related cushion layers are also compared and discussed. Corresponding conclusions were drawn based on the outcomes of the investigation.

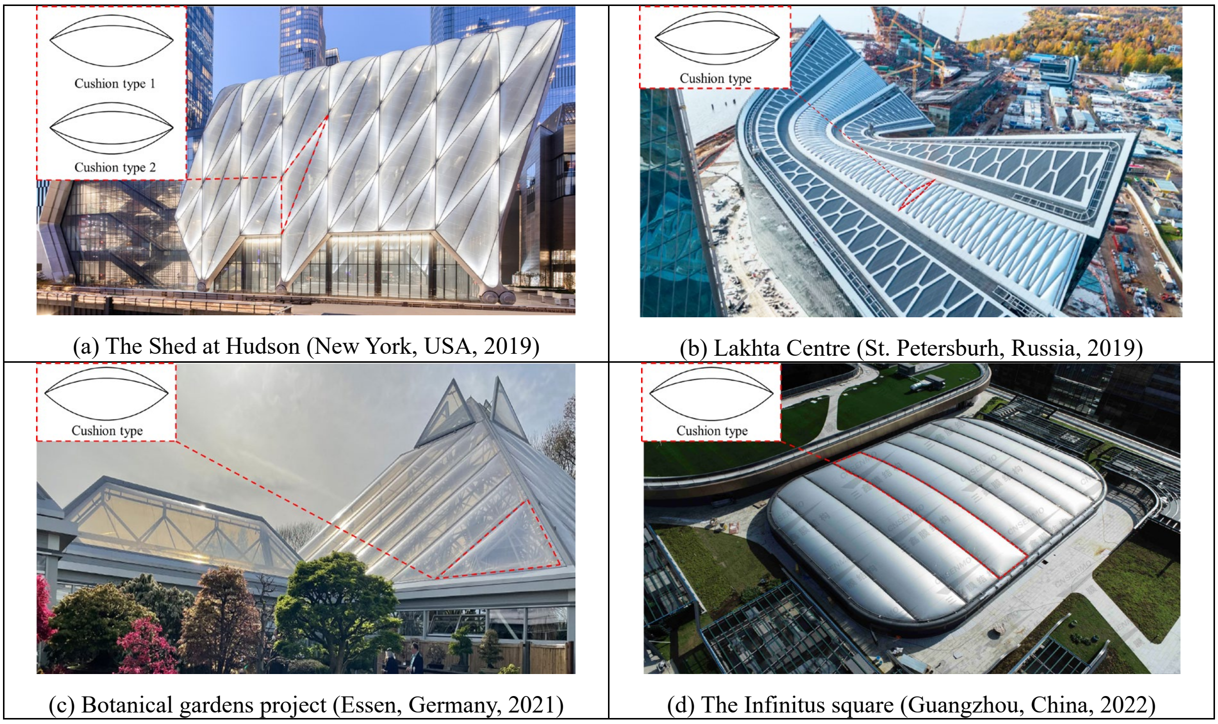

(a) The Shed at Hudson (New York, USA, 2019)
(b) Lakhta Centre (St. Petersburh, Russia, 2019)
(c) Botanical gardens project (Essen, Germany, 2021)
(d) The Infinitus square (Guangzhou, China, 2022)

Figure 3. Multiple-layer ETFE cushion engineering projects

2. Experimental system and test procedures

2.1 ETFE cushion specimen

As depicted in Figure 4, two specimens were fabricated with three ETFE foils with thickness of 250 μ m, 150 μ m and 250 μ m, respectively. To accommodate the size limitations of the load simulation compartment (LSC), the planar dimensions of the ETFE cushions were set at 1500 mm × 1500 mm. The initial rise of 188mm and cushion’s shape were achieved using the specialized lightweight structure design and analysis software, EASY version 2023[12], based on the designated internal pressure. Meanwhile, the middle layer was adjusted to a height of 127 mm, constituting roughly 67% of the cushion's total height to create a gap chamber with the top layer. To ensure a smooth surface for the ETFE cushion specimens, The patterning is based on the form founding surface and three-dimensional (3D) patterning method was employed.

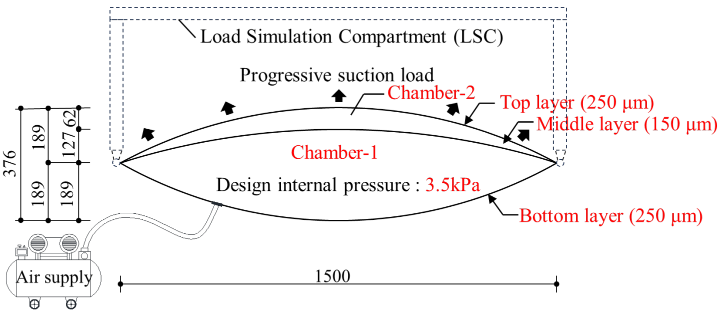

Figure 4. Structural scheme of tri-layer ETFE cushion specimens

As the air supply chamber, chamber-1 is designed to operate at a working pressure of 3.5 kPa. This design results in an approximate stress level of 10 MPa on the external cushion layers, a value that falls below the first yield point of ETFE foils and closely aligns with engineering applications.

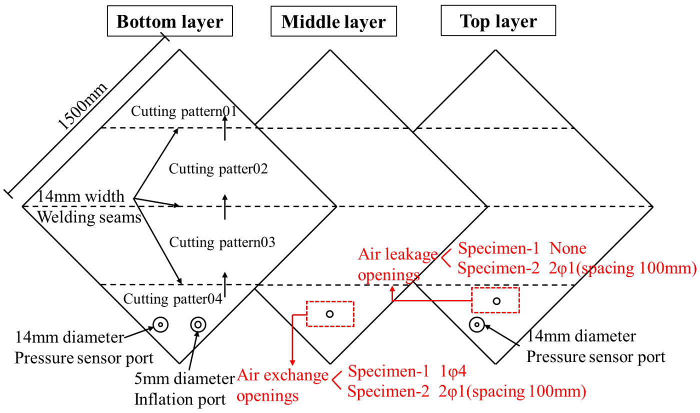

Figure 5. opening information on ETFE cushion specimens

Two square tri-layer and two-chamber ETFE cushion specimens with distinct air-exchange openings and air-leakage openings were meticulously designed and manufactured. As shown in Figure 5 and Figure 6, specimen-1 featured a single 4mm diameter air exchange opening (1 Φ 4) positioned in the corner region of the middle layer, which aims to acquire equal pressure among two chambers. For specimen-2, two 1mm diameter micro-openings (2 Φ 1) were created by a pin at the corner of the middle layer and the top layer, each spaced 100mm apart. It is to generate an air leakage flow throughout the cushion structure and enable the middle layer to acquire design shape.

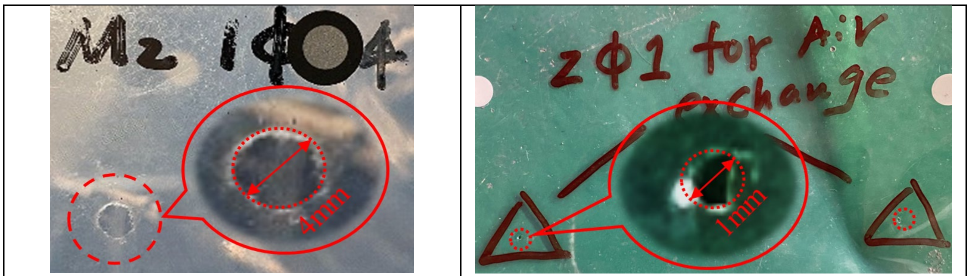

(a) 1φ4 air-exchange opening on specimen 1 (b) 2φ1 air-exchange opening on specimen 2

Figure 6. Air-exchange opening design on specimens

2.2 Load simulation system

The load simulation system consisted of Load Simulation Compartment (LSC) and an Automatic pressure control subsystem.

As shown in Figure 7, the LSC had dimensions of 1863 mm × 1703 mm × 1600 mm, constructed using rectangular hollow section (RHS) steel and steel plates. It was further reinforced with two-way stiffener steel plates to ensure a maximum bearing capacity of 50 kPa of air pressure. As vacuum degree of the LSC adjusted under control, it allows for the uniform application of suction or pressure loads on the ETFE cushion in the normal direction.

To meet the experimental requirements of high pressure, high precision, and rapid response, a specialized automatic pressure control subsystem was developed. To achieve the desired system functionality, pressure sensors, a Pressure Measure and Control Unit (PMCU)[13], an air compressor, a vacuum pump, multiple solenoid switching valves, and a computer were utilized. The internal pressure of specimen chamber-1 and the LSC was continuously monitored by pressure sensors and transmitted to the PMCU. Based on the measured pressure and the pressure control program, the PMCU generated actuation commands for the solenoid switching valves. These commands were then executed by the valves to achieve inflation or deflation for cushion chamber-1 and pumping or holding for the LSC, thereby allowing precise adjustment and control of the pressure as needed.

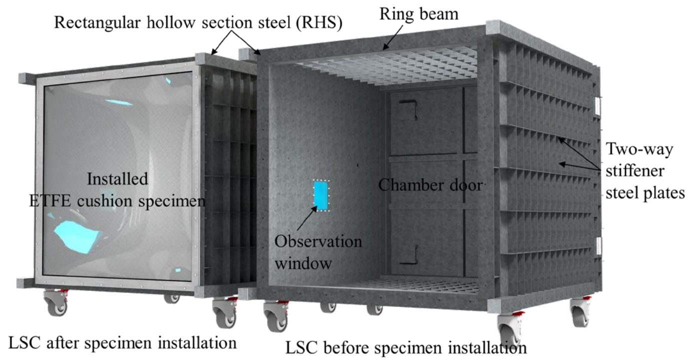

Figure 7. Structural scheme of Load Simulation Compartment (LSC)

2.3 Measurement subsystem

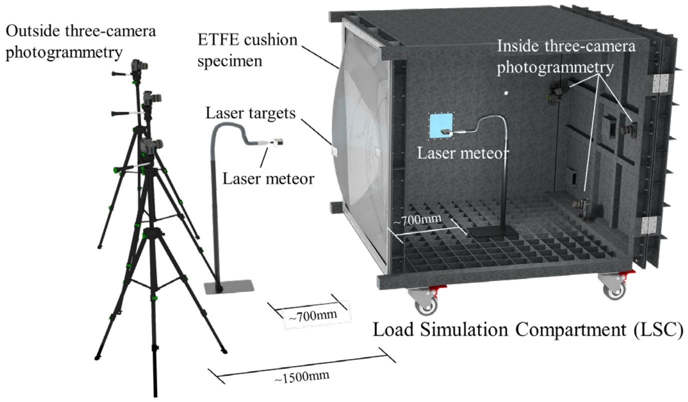

Figure 8. Deployment scheme of measurement subsystem

A visual representation of the measurement subsystem deployment scheme is presented in Figure 8. To measure the surface height variation of the specimen’s external surfaces, two laser targets were glued at the geometric center of the double-outer-layer. Two laser meteors were positioned approximately 700mm away from the cushion surfaces detect the displacement of these targets.

An optical measurement subsystem was employed to obtain the geometric shape of cushion. This subsystem consisted of six cameras with wireless remote-control equipment, placed in front and back side of the specimens. 196 reflective targets, each with a 5mm ($\Phi 5$) diameter, were pasted on each surface in a 16×16 array with 100mm row and column spacing. These reflective targets can reflect camera flashes and captured by the cameras. Images of the reflective targets at each load step would be processed in PhotoModeler Premium 2020[14], where the reflective targets within the images were identified as point cloud and whose special coordinates could be calculated and acquired, the geometric information of each layer was therefore obtained.

2.4 Experimental procedures

As shown in Figure 9, the cushion specimen was firstly inflated at a rated inflation rate of 0.83kPa/min until pressure of chamber-1 reached 3.5kPa, which was then maintained continuously. Subsequently, suction loads were incrementally applied in steps of -1 kPa, with a rate of increase set at 1.15 kPa/min. Each suction load step was sustained for a duration of 20 minutes, allowing the cushion to deform steadily, and facilitating data recording. To ensure a comprehensive observation of the specimen's failure process, the suction load would be continually increased without maintaining at 30kPa until the specimen reaches failure.

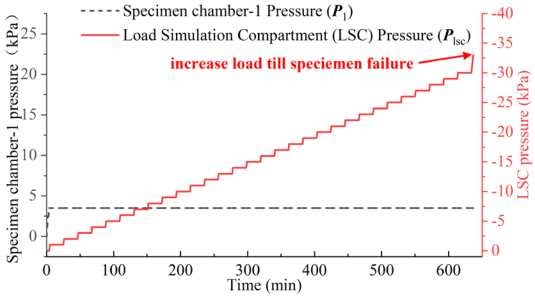

Figure 9. Suction loading scheme

3. Result and discussions

3.1 Structural deformation

3.1.1 Surface height

The analysis of structural deformation is of great importance for evaluating structural behaviours. The surface height variation of the top layer and the middle layer is measured by the laser meteors and the result is plotted in Figure 10. As the suction load increased, both top layer and middle layer of specimen-2 deform with rapid increase on surface height and merge in the end. While for specimen-1, only the top layer undergoes significant deformation, with minimal deformation observed from middle layer. This phenomenon indicates that both layers of spciemn-2 share load together and commonly deform as suction load increases, while for specimen-1, it is only the top layer performs substantial deformation.

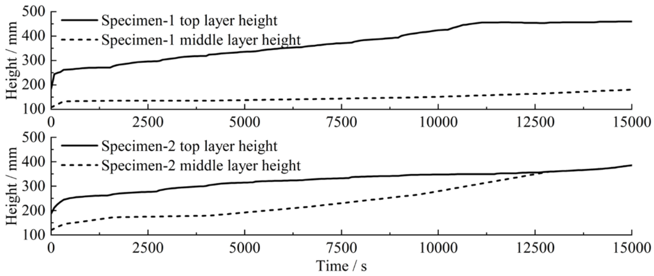

Figure 10. Surface height variance of specimens

For an identical ETFE film under short-term static suction load, greater deformation is highly related to greater applied load. Therefore, different deformation trend observed from two identical specimens mostly implied different load distribution among layers. In Figure 11, specimen-2 shows a considerably lower magnitude in top surface height but a greater middle surface height than specimen-1 under identical load. It implies that less distributed load on the top layer while greater distributed load on the middle layer for double-outer-layer of specimen-2.

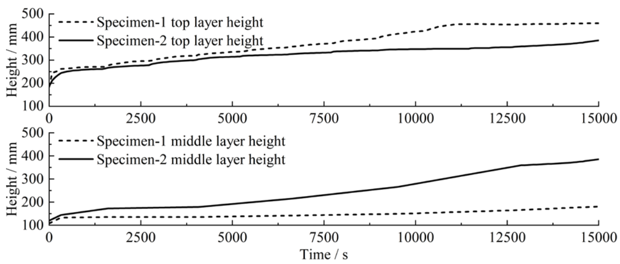

Figure 11. Surface height variation difference of top layer and middle layer

3.1.2 Geometric shape

The optical measurement result shows the same deformation phenomenon and reach in good alignment. Different from laser meteors, optical measurements can help rebuild in-situ target layer surface and provide more visual deforming information.

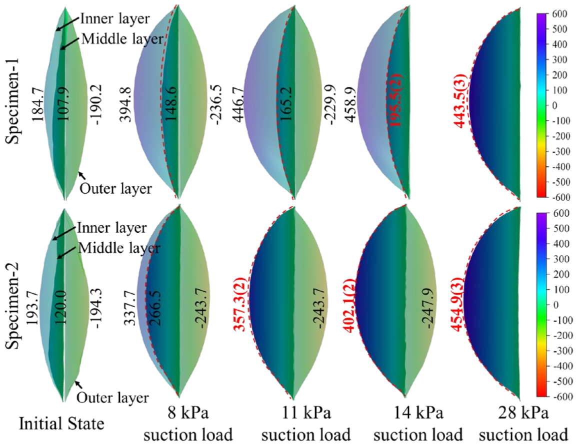

Figure 12. Structural deformation and surface height of specimens under suction load (Unit: mm)

The cushion shape under five load steps were processed and depicted in Figure 12. A clear distinction in structure deforming process is observed for two specimens, especially for double-outer-layer. Commonly, both two specimens perform similar deforming trend, three layers deform in the loading direction and adhered together ultimately. However, compared to specimen-1, specimen-2 exhibits smaller deformation on the top layer but substantial deformation on the middle layer. The double-outer-layer of specimen-2 deforms consistently and adheres firstly at 11kPa. While the double-outer-layer of specimen-1 keep separating as load intensified. Different deforming trend of double-outer-layer raise different structure deformation. As the double-outer-layer performing highly consistent deformation for specimen-2, The cushion structure was induced smaller overall deformation and capable to maintain cushion shape under greater load. To some extent, the load carrying performance is enhanced as the cushion performs less deformation under identical suction load.

3.2 Load distribution

As for tri-layer and two-chamber ETFE cushion, the load distribution on double-outer-layer determines the withstanding air pressure and working stress of each layer. It thus largely affects the structural deformation and overall structural performance. Force analysis is an easy and convenient way to gain loading situation of target layers.

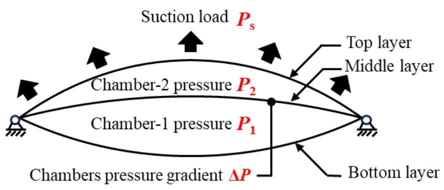

Figure 13. Principle force diagram of tri-layer and two-chamber cushion structure

Figure 13 shows the principal force diagram of a tri-layer and two-chamber ETFE cushion under suction load. Distributed pressure applied on the top layer can be naturally expressed as:

$$\boldsymbol{P_{TL} = P_2 + P_s} \tag{1}$$

And the distributed pressure on the middle layer can be defined as follows:

$$\boldsymbol{P_{ML} = P_1 - P_2 = \Delta P} \tag{2}$$

Here, the pressure of chamber-2($\boldsymbol{P_2}$) can be expressed as:

$$\boldsymbol{P_2 = P_1 - \Delta P} \tag{3}$$

Finally, for the top layer, whose bearing pressure can be described as:

$$\boldsymbol{P_{TL} = P_s + P_1 - \Delta P} \tag{4}$$

3.2.1 Middle layer

Instead of bearing external load directly, the middle layer withstands the pressure gradient(difference) of two chambers. The greater pressure gradient, the greater surface deformation and surface stress. Consequently, it brings potential structural stiffness enhancement and decreased overall structure deformation.

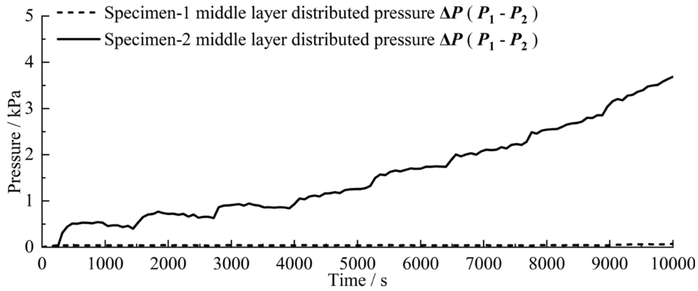

Figure 14. Chambers pressure gradient curve

As shown in Figure 14, specimen-2 exhibits a rapid increase in chambers' pressure gradient as suction load intensifies, whereas no such development is observed for specimen-1. This strongly explains the noticeable deformation of the middle layer for specimen-2. Micro-openings on double-outer-layer trigger limited gas exchange rate between chambers, it then causes sharp decrease of chamber-2's pressure and increase of chamber pressure gradient under progressive suction load. Therefore, it becomes reasonable for specimen-2 to perform greater middle layer deformation.

3.2.2 Top layer

As for double-outer-layer in this study, top layer is the most crucial layer as it withstands the external influence directly. The deformation and the mechanical performance of the top layer is of great importance for structural safety and strength.

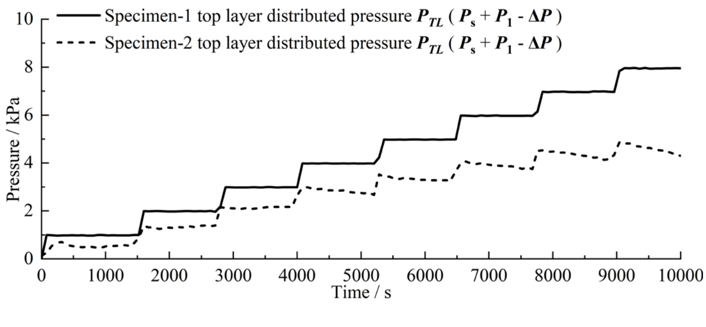

Figure 15. Curve of distributed load on top layer

The curve of distributed load on top layer for two specimens is plotted in Figure 15. The distributed load of the top layer exhibits a stepwise increase, with specimen-2 demonstrating a clearly lower magnitude than specimen-1. It is because the growth of pressure gradient between chambers is greater for specimen-2 and the distributed load on top layer is therefore decreased. With greater chamber pressure gradient and less bearing load, greater deformation on middle layer and less on top layer becomes reasonable.

Obviously, when pressures are equalized in both chambers ($\Delta \boldsymbol{P} = \mathbf{0}$), the entire suction load is applied solely to the top layer along with internal pressure $\boldsymbol{P_1}$, while the middle layer remains unloaded. The double-outer-layer separates as suction load intensified, performing significant deformation on cushion shape. However, when a pressure gradient ($\Delta \boldsymbol{P} > \mathbf{0}$) is induced between the chambers, there is a decrease of $\Delta \boldsymbol{P}$ on bearing pressure of the top layer and $\Delta \boldsymbol{P}$ increase on the middle layer. The double-outer-layer deform consistently and withstand load together, exhibiting smaller overall deformation. In other words, the pressure gradient can help adjust the distributed load over double-outer-layer and enable both layers to collaborate in bearing load and work in a tandem. It helps decrease the deformation of the entire structure and show structural stiffness enhancement.

4. Ultimate bearing capacity and failure mode

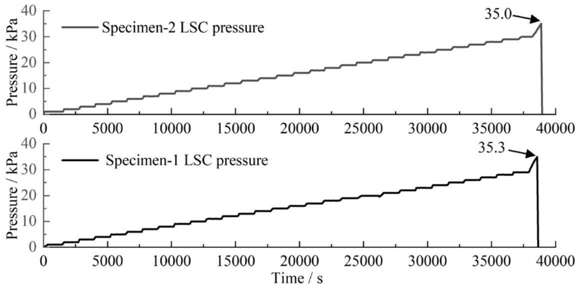

Figure 16. LSC pressure variation of two specimens

The ultimate bearing capacity and failure mode are important parameters for structural safety evaluation of cushion structure. While the ultimate bearing capacities of specimen-1 and specimen-2 are closely matched at 35.3 kPa and 35.0 kPa, respectively, their failure modes exhibit significant differences, as depicted in Figure 16 and Figure 17. Specimen-1 experienced sudden and dramatic destruction, marked by a loud noise, as tearing occurred along the top edge, resulting in a noticeable 1484 mm long tearing slit. Conversely, specimen-2 exhibited a layer-by-layer progressive failure at the central area. In this case, all layers underwent similar tearing destruction perpendicular to the welding seams, resulting in a tearing slit.

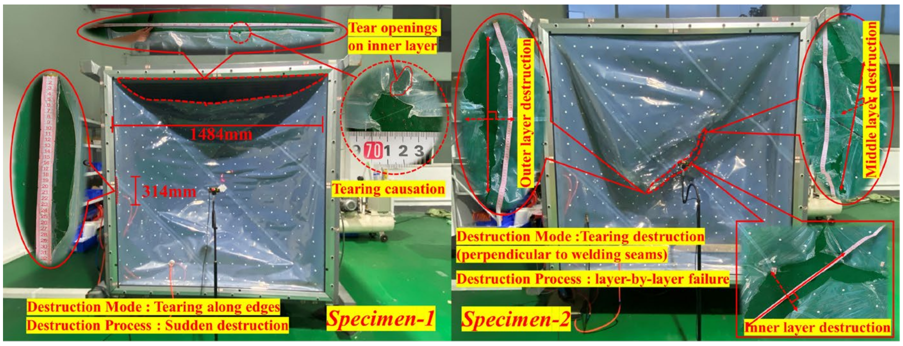

Figure 17. Failure mode of specimens

5. Conclusions

This study experimentally investigates the structural behaviour of the tri-layer and two-chamber ETFE cushion at the first time. With different film opening design, two specimens demonstrate distinct chamber pressure responses and structural behaviours, establishing a strong correlation between these factors. The influencing mechanism is comprehensively discussed, aligning well with experimental results. The ultimate performance of both tri-layer and two-chamber configurations is meticulously recorded and analysed. The subsequent sections provide key conclusions drawn from the study:

1. The chamber pressure gradient plays a crucial role in ensuring the proper functionality of the double-outer-layer. This chamber pressure gradient assists in adjusting the distributed load across the double-outer-layer, allowing both layers to collaborate in bearing the load and work in tandem.

2. The normal functionality of the double-outer-layer can help enhance the structural performance, particularly in reducing the overall deformation of tri-layer and two-chamber ETFE cushions under identical suction loads

3. The chamber pressure gradient has no impact on the ultimate bearing capacity but induces a shift in the failure mode. The ultimate bearing capacity of two specimens is approximately 35kPa. Specimen-1 exhibits sudden and dramatic destruction with a long tearing slit, while specimen-2 exhibits a layer-by-layer progressive failure at the central area.

This study represents the first experimental investigation into the structural behaviour of tri-layer and two-chamber ETFE cushions, identifying the key factor that influences the functionality of the double-outer-layer. These findings offer valuable insights into the understanding of performance enhancement mechanisms and provide inspiration for further research in this field

6. Acknowledgements

This work was supported by the National Natural Science Foundation of China (Grant. 52278191). The experimental ETFE cushion specimens were produced by Shanghai Taiyo Kogyo Co. Ltd. These supports are gratefully acknowledged by the authors.

References

[1] T. Tanigami, K. Yamaura, S. Matsuzawa, M. Ishikawa, K. Mizoguchi, and K. Miyasaka, “Structural studies on ethylene-tetrafluoroethylene copolymer: 2. Transition from crystal phase to mesophase,” *Polymer*, vol. 27, no. 10, pp. 1521–1528, 1986, doi: 10.1016/0032-3861(86)90098-4.

[2] S. Robinson-Gayle, M. Kolokotroni, A. Cripps, and S. Tanno, “ETFE foil cushions in roofs and atria,” *Construction and Building Materials*, vol. 15, no. 7, pp. 323–327, 2001, doi: 10.1016/S0950-0618(01)00013-7.

[3] W. Chen, “Design of membrane structure engineering,” *China Building Industry Press, Beijing*, 2005.

[4] L. Charbonneau, M. A. Polak, and A. Penlidis, “Mechanical properties of ETFE foils: Testing and modelling,” *Construction and Building Materials*, vol. 60, pp. 63–72, 2014, doi: 10.1016/j.conbuildmat.2014.02.048.

[5] J. Hu, W. Chen, B. Zhao, and D. Yang, “Buildings with ETFE foils: A review on material properties, architectural performance and structural behavior,” *Construction and Building Materials*, vol. 131, pp. 411–422, 2017, doi: 10.1016/j.conbuildmat.2016.11.062.

[6] A. LeCuyer, *ETFE: technology and design*. Walter de Gruyter, 2008.

[7] L. A. Robinson, “Structural Opportunities of ETFE,” p. 66, 2005.

[8] “The Shed at Hudson Yards,” Vector Foiltec. Accessed: Nov. 26, 2023. [Online]. Available: https://www.vector-foiltec.com/projects/the-shed-design-concepts/

[9] “Lakhta Center,” Taiyo Europe. Accessed: Nov. 26, 2023. [Online]. Available: https://taiyo-europe.com/?taiyo-portfolio=lakhta-center

[10] “Grugapark Essen Conservatories,” Vector Foiltec. Accessed: Nov. 26, 2023. [Online]. Available: https://www.vector-foiltec.com/projects/grugapark-essen-conservatories/

[11] “The Infinitus suqare ETFE membrane projects, Guangzhou.” Accessed: Nov. 26, 2023. [Online]. Available: http://www.senmo.com.cn/index.php?m=Show&a=index&cid=13&id=84

[12] “Software for Form Finding, Statics and Cutting Pattern Generation of membrane- and cable net structures.” Accessed: Nov. 28, 2023. [Online]. Available: https://www.technet-gmbh.com/en/products/easy/

[13] B. Zhao *et al.*, “An automatic system for pressure control and load simulation of inflatable membrane structure,” *AUTOMATION IN CONSTRUCTION*, vol. 90, pp. 58–66, 2018, doi: 10.1016/j.autcon.2018.02.022.

[14] “PhotoModeler Premium – PhotoModeler.” Accessed: Nov. 28, 2023. [Online]. Available: https://www.photomodeler.com/products/premium/